AIP | Applied Physics Letters

Patchy Janus particles with tunable roughness and composition via vapor-assisted deposition of macromolecules

Kimberly B. Shepard, Dane A. Christie, Chris L. Sosa, Craig B. Arnold, and Rodney D. Priestley

Citation: Applied Physics Letters **106**, 093104 (2015); doi: 10.1063/1.4913913
View online: http://dx.doi.org/10.1063/1.4913913
View Table of Contents: http://scitation.aip.org/content/aip/journal/apl/106/9?ver=pdfcov
Published by the AIP Publishing

Patchy Janus particles with tunable roughness and composition via vapor-assisted deposition of macromolecules

Kimberly B. Shepard,[1] Dane A. Christie,[1] Chris L. Sosa,[1] Craig B. Arnold,[2,3] and Rodney D. Priestley[1,3,a)]
[1]Chemical and Biological Engineering Princeton University, Princeton, New Jersey 08544, USA
[2]Mechanical and Aerospace Engineering Princeton University, Princeton, New Jersey 08544, USA
[3]Princeton Institute for the Science and Technology of Materials, Princeton University, Princeton, New Jersey 08544, USA

(Received 24 November 2014; accepted 19 February 2015; published online 2 March 2015)

Here, we present a technique for the fabrication of patchy Janus particles utilizing a vapor-assisted macromolecular deposition technique, termed Matrix Assisted Pulsed Laser Evaporation (MAPLE). Using this technique, both inorganic and organic precursor particles, immobilized on a surface, are functionalized on one hemisphere with nanodroplets of a desired polymer, thus forming particles with a patchy Janus morphology and textured surface topology. This fabrication method is flexible with respect to the chemical identity of the precursor particle and the selection of the deposited polymer. By tuning MAPLE deposition parameters, e.g., target composition or deposition time, the Janus anisotropy and roughness (i.e., patchiness) can be tuned, thus enabling greater control over the particles' behavior for applications as nanoparticle surfactants for stabilization of emulsions and foams. © *2015 AIP Publishing LLC*. [http://dx.doi.org/10.1063/1.4913913]

Janus particles, which incorporate two or more "faces" with different chemical functionality, have been the subject of great interest since P. G. de Gennes discussed their vast application potential in his 1991 Nobel prize lecture.[1] Janus particles can be fabricated from organic and/or inorganic materials in an array of geometries, including spheres, dumbbells, rods, and shells.[2] Applications of Janus particles are correspondingly diverse, for example: as particles active at interfaces,[3–5] emulsion stabilizers,[6–9] optically active materials,[10,11] self-propelling particles,[12] and in biological applications.[13–16] Among the numerous Janus particle synthetic techniques, one of the most common is a masking technique in which a mono-functional precursor particle is selectively decorated with a second material. In this method, a 2-D array of the precursor particles is immobilized, then temporarily covered or protected on one side only, thus breaking the symmetry of the precursor particles.[2,17] In this way, a second material phase can be applied to the immobilized precursor particles on the exposed side, thus forming a Janus particle.[18–20] In cases where the second material is applied via a directional deposition method, e.g., physical vapor deposition (PVD), the substrate can act as an effective mask. An advantage of this family of synthetic techniques is that it enables the fabrication of Janus particles with diverse material combinations: it is feasible to vary both the chemical identity of the precursor particle and the second coating material.[2,18]

For 2D synthetic techniques, there exist opportunities for improving the generality and simplicity of material deposition. Regarding the former, the use of PVD in the fabrication of Janus particles limits the selection of the coating layer to atomic and molecular systems. A result is that polymer-polymer Janus particles cannot be fabricated using PVD. The range of coatings can be expanded to polymeric materials by the application of CVD or plasma-polymerization. These techniques require specific functional groups and reaction conditions to enable the simultaneous polymerization and deposition of macromolecules.[2,21–24] Regarding the latter, certain 2D fabrication approaches require multiple processing steps after precursor particle immobilization, such as coating with a chemically appropriate mask layer, etching the mask, chemical functionalization, and selective removal of the mask prior to removal of Janus particles from the substrate.[20] Here, we report the utility of a unique vapor-assisted deposition process to generate both polymer-inorganic and polymer-polymer Janus particles via the 2D scheme. In this approach, the deposition of the polymer-coating layer is achieved in the absence of polymerization. Only one processing step is required between immobilization and particle release. We demonstrate a versatile process for the fabrication of Janus nanoparticles for broad application in the supramolecular assembly of nanostructured materials,[25] solution-dispersed interfacial stabilizers,[26] and targeted drug-delivery vehicles.[27] Uniquely, we are able to control both the surface roughness (patchiness) and particle anisotropy without adding additional complexity to the fabrication process.

The enabling technology for the Janus particle fabrication process presented here is Matrix Assisted Pulsed Laser Evaporation (MAPLE), a laser-based deposition technique, used to create thin films or nanodroplets of polymers, proteins, nanoparticles, and nanocomposites.[22,28] Owing to the technique's growing popularity since its invention in the late 1990s,[29] MAPLE systems are now commercially available.[30] Recently, we have demonstrated that MAPLE can be used to directionally deposit polymer nanodroplets[31] onto an arbitrary substrate. Briefly, in the MAPLE technique, a pulsed laser strikes a frozen target made from a dilute polymer solution, inside a high vacuum chamber. The interaction between laser and target material causes nano- to micro-size droplets

a)Author to whom correspondence should be addressed. Electronic mail: rpriestl@princeton.edu.

of polymer and solvent to be ejected towards the substrate. During flight from target to substrate, the solvent evaporates and the remaining polymer droplets are collected atop a temperature-controlled substrate. At high substrate temperatures, polymer droplets coalesce to create a smooth film. We take advantage of the deposition process to create Janus particles. In this way, polymer nanodroplets and films are MAPLE-deposited onto the target-facing side of a precursor particle film. Because MAPLE is a line-of-sight deposition process, only the exposed halves of the particles are coated. The result is the formation of patchy Janus particles.

Analogous to other 2D fabrication techniques, a monolayer of precursor particles is necessary to ensure that the depositing material contacts only one hemisphere of the particles. In order to create Janus particles by MAPLE, a uniform monolayer is used as an effective substrate upon which polymer nanodroplets are deposited. After MAPLE deposition, the fabricated Janus particles can be removed from the substrate into a suspension by gentle sonication. In principle, micro and nanosize particles of any composition can be used as precursor particles, so long as a technique exists to immobilize the particles into a monolayer on a flat substrate. We demonstrate the technique's versatility by utilizing both organic (350 nm polystyrene) and inorganic (700 nm silica) spheres as precursor particles. This MAPLE-based fabrication technique is also flexible with respect to precursor particle size, the only requirement being that the precursor particle must be larger than the deposited polymer nanodroplets to prevent particle aggregation. Based on our prior investigate of the early-stage morphology of MAPLE-deposited films,[31] precursor particles of greater than 100 nm in diameter are feasible candidates for this technique. We further emphasize the technique's broad applicability by demonstrating the deposition of two different polymers, poly(methyl methacrylate) (PMMA) and poly(ethylene oxide) (PEO), onto silica precursor particles.

For both silica and polystyrene precursor particles, a close-packed colloidal monolayer was prepared on a silica substrate via a convective assembly technique utilizing drag coating from a methanol/water solution.[32] A detailed experimental protocol and typical laser scanning confocal microscope image of a monolayer of precursor silica particles over a 50 μm area are included in the supplementary material.[33] Amorphous PMMA or semicrystalline PEO were MAPLE-deposited onto glass substrates coated with a precursor particle monolayer. A schematic of the MAPLE-deposition process is shown in Figure 1. Atomic force microscopy (AFM) was used to characterize the resulting polymer-decorated precursor particles. Figures 2(a) and 2(b) show height and phase images, respectively, of 700 nm diameter PMMA/silica patchy Janus particles fabricated by MAPLE. The PMMA polymer partially wets the silica surface, forming rounded nanodroplets ranging from tens to hundreds of nanometers in size. The small size of the nanodroplets relative to the precursor particles ensures the formation of patchy Janus particles with high patchiness. The small droplet size also lowers their probability for forming polymer bridges between two precursor particles.

Figures 2(c) and 2(d) show AFM height and phase images for 350 nm PMMA/PS patchy Janus nanoparticles prepared via MAPLE. These particles differ from those shown in Figures 2(a) and 2(b), in both precursor particle size (350 nm vs. 700 nm) and precursor particle chemical identity (PS vs. silica). Despite a twofold difference in precursor particle size and dissimilar chemical identity when compared with Figures 2(a) and 2(b), a similar morphology is obtained for the PMMA/PS Janus particles. These results show that the size and precursor particle material can be varied without substantially changing the resulting patchy Janus morphology. Figures 2(e) and 2(f) show AFM height and phase images of PEO/silica patchy Janus particles prepared in the same manner. A similar, but not identical morphology

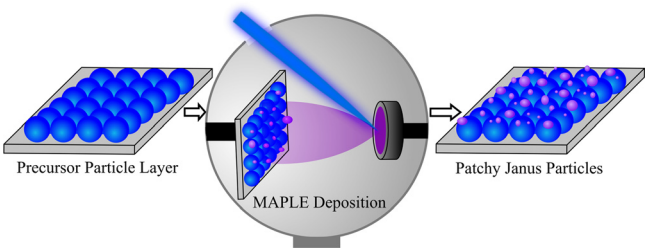

FIG. 1. Schematic of patchy Janus particle fabrication via MAPLE deposition.

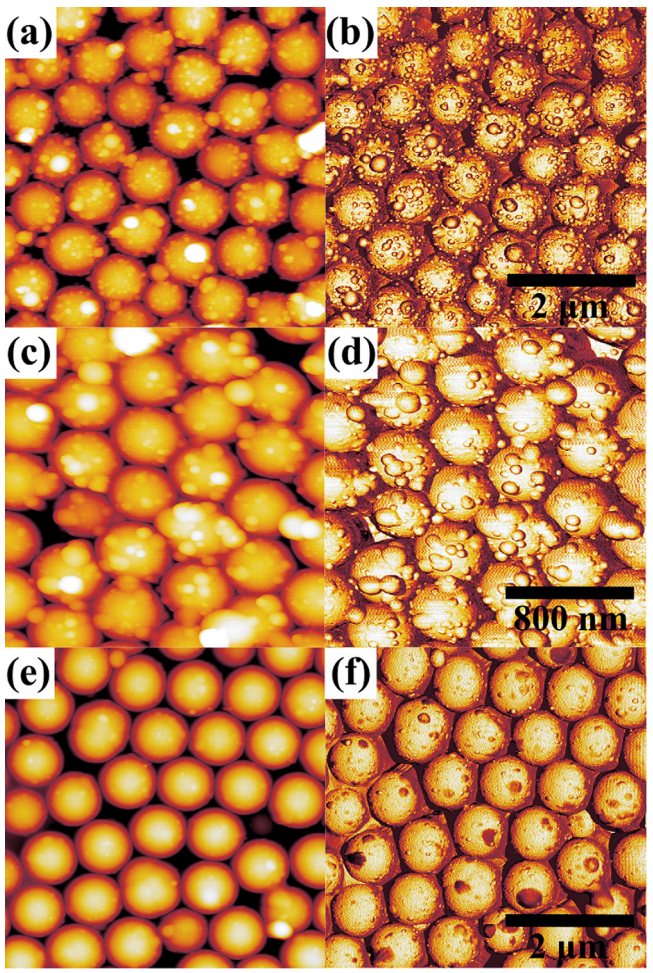

FIG. 2. Atomic force microscopy height (a) and phase (b) images of 700 nm patchy PMMA/silica Janus particles. Height (c) and phase (d) images of 350 nm patchy PMMA/polystyrene Janus particles (note smaller scale bar from (b) and (f)). Height (e) and phase (f) images of 700 nm PEO/silica patchy Janus particles.

is observed with smaller, flatter nanodroplets, some of which appear dark in the phase image. We attribute the dark nanodroplets to amorphous, rubbery regions in the semicrystalline PEO polymer. The difference in contact angle between PEO and PMMA nanodroplets is likely due to the difference in the glass transition temperature (T_g) of the two materials. During processing, PEO is far above its T_g, meaning the polymer comes into contact with the precursor particle as a liquid, enabling the droplets to reach an equilibrium contact angle. In contrast, PMMA is far below its T_g, vitrifying into the glassy state upon contact with the precursor particle, becoming trapped in a non-equilibrium state with a higher contact angle. Other work in our group on similar nanodroplets has shown that upon high temperature annealing, the contact angle of the PMMA approaches that observed for PEO.[34] Combined, these three depositions demonstrate that this technique can be used to preferentially decorate one side of a various of precursor particles with nanodroplets of different polymers to form patchy nanostructured Janus particles.

The MAPLE technique affords control over numerous process variables that can be employed to tailor the morphology of the resulting Janus particles. We demonstrate the ability to control and tailor the morphology of PMMA/silica patchy Janus particles. The MAPLE deposition time is a straightforward variable to manipulate and proportionally controls the amount of material which is deposited onto the precursor particles. Figure 3 summarizes the effect of deposition time (5, 10, and 30 min) on PMMA decoration onto silica precursor particles, and hence patchy Janus particle composition. Though it is clear to the eye that longer deposition times result in more polymer nanodroplets deposited atop the precursor particles, a quantification of the trend is warranted. In previous work, we utilized image-processing software to characterize the fractional coverage and size distribution of nanodroplets deposited via MAPLE onto flat silica substrates. We found that after ~10 min of deposition, the size distribution remains constant.[31] Here, we estimate the relative composition of the patchy Janus particles by calculating the fractional area of the AFM phase image occupied by polymer nanodroplets. Using this technique, we find that the fractional area scales approximately linearly with deposition time, accounting for experimental error and small sample size, in which the presence of one large nanodroplet in an image can significantly change area occupied by polymer. Approximately 2% of Figure 3(b) (5 min deposition) is occupied by polymer nanodroplets. When the deposition time is doubled to 10 min (see Figure 3(d)), the area occupied by polymer nanodroplets also doubles to 4%. 30 min of MAPLE deposition (see Figure 3(f)) further increases the polymer nanodroplet fraction to ~17%. By varying the deposition time, the Janus anisotropy can be systematically controlled.

For the use of Janus particles at interfaces and in emulsions, it has been demonstrated that the size, shape, and surface characteristics of patchy particles are crucial for tailoring material attributes to application requirements.[35,36] To that end, we show that by adjusting the temperature of the precursor particle substrate during MAPLE deposition, the surface area, i.e., roughness, of the PMMA depositing

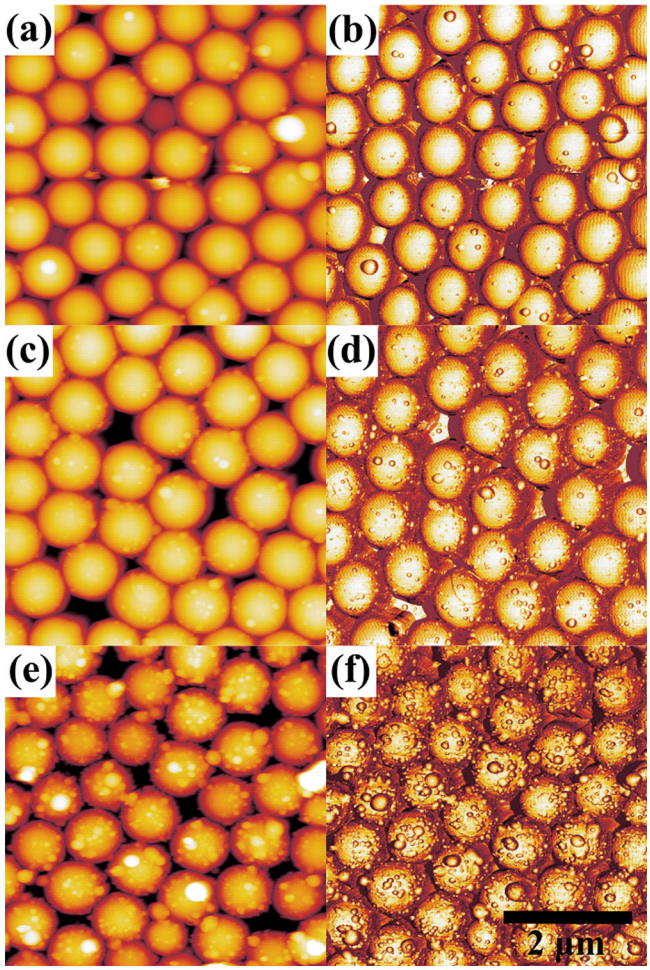

FIG. 3. Height (left column) and phase (right column) images of patchy PMMA/silica Janus particles with increasing MAPLE deposition time: 5 min ((a) and (b)), 10 min ((c) and (d)), and 30 min ((e) and (f)).

phase can be controlled independently from the Janus anisotropy. The glass transition temperature (T_g) of the PMMA is ~85 °C. At substrate temperatures (T_{sub}) below the T_g of PMMA, the roughness of the PMMA phase is independent of the deposition temperature. Therefore, the AFM images of particles fabricated at $T_{sub} = 27$ °C (see Figures 4(a) and 4(b), same as Figures 3(e) and 3(f)) are representative of the sub-T_g morphology. At temperatures just above the T_g, ($T_{sub} = 90$ °C, Figures 4(c) and 4(d)), the roughness begins to decrease. Fewer small nanodroplets, i.e., those with diameter ~10–30 nm, are visible in the AFM image as they have flattened. Some polymer droplets which contact more than one particle begin to form bridges between the particles. Deposition at $T_{sub} = 110$ °C (see Figures 4(e) and 4(f)), causes most nanodroplets to wet the precursor particle's surface, with only a few larger nanodroplets remaining visible. At the highest deposition temperature, $T_{sub} = 130$ °C (see Figures 4(g) and 4(h)), the deposited PMMA coalesces into a single droplet on the particle face with a low contact angle. It is important to note that the deposited material appears to remain on the front side of the precursor particles even at high deposition temperatures. This is in contrast to the behavior of Janus particles fabricated with $T_{sub} = 27$ °C and then annealed for 1 h at 130 °C (see supplementary material, Fig. S2 (Ref. 33)). Under these conditions, polymer

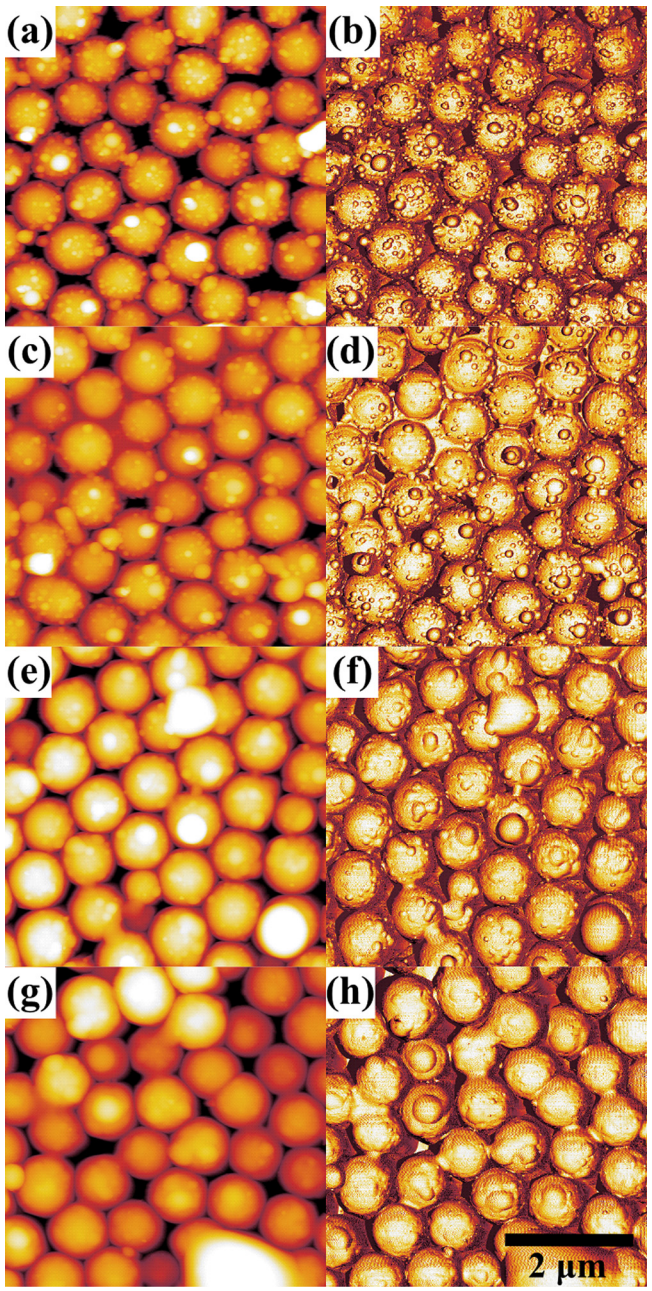

FIG. 4. Height (left column) and phase (right column) images of PMMA/silica patchy Janus particles fabricated at various substrate temperatures: 27 °C ((a) and (b)), 90 °C ((c) and (d)), 110 °C ((e) and (f)), and 130 °C ((g) and (h)). Surface roughness of the patchy PMMA phase decreases with increasing substrate temperature.

molecules diffused to the substrate or formed bridges between the particles, thus effectively eliminating the Janus morphology. We hypothesize that the gradual deposition of polymer during the MAPLE process enables the liquid polymer droplets to remain on the forward-facing side of the nanoparticles. Only the polymer which is deposited in the first few laser pulses of deposition spends 30 min at elevated temperature, all subsequent polymer is exposed to high temperature for proportionally less time. As demonstrated, the control of substrate temperature relative to the depositing material's T_g during MAPLE deposition represents a straightforward approach to direct the resulting Janus particle surface roughness.

Regardless of their intended application, processing of Janus particles typically includes their suspension in liquid, therefore it is important to characterize the Janus particles after removal from the substrate via sonication into water. A 2 cm^2 piece of glass substrate with PMMA/silica patchy Janus particles was immersed in 2 ml deionized water and placed in a sonic bath for 5 min. The process resulted in the formation of a cloudy liquid suspension. Both AFM and SEM were employed to confirm the Janus morphology after the particle release step. In Figures 5(a) and 5(b), two SEM images of particles (sputtered with 5 nm of Iridium) with the Janus morphology are shown. The SEM images show examples of PMMA/silica patchy Janus particles with both coated and uncoated hemispheres visible. AFM height (Figs. 5(c) and 5(e)) and phase images (Figs. 5(d) and 5(f)) agree with the SEM images, showing both of the Janus particle hemispheres. Together, the AFM and SEM images confirm that the PMMA nanodroplets remain intact after removal from the substrate by sonication, thus preserving the Janus structure. The PMMA/silica Janus particles are also shelf stable: particles for the AFM and SEM images were dropcast from the same suspension, 2 months apart. Brief agitation on a vortex mixer was sufficient to re-suspend the particles for drop casting prior to SEM imaging.

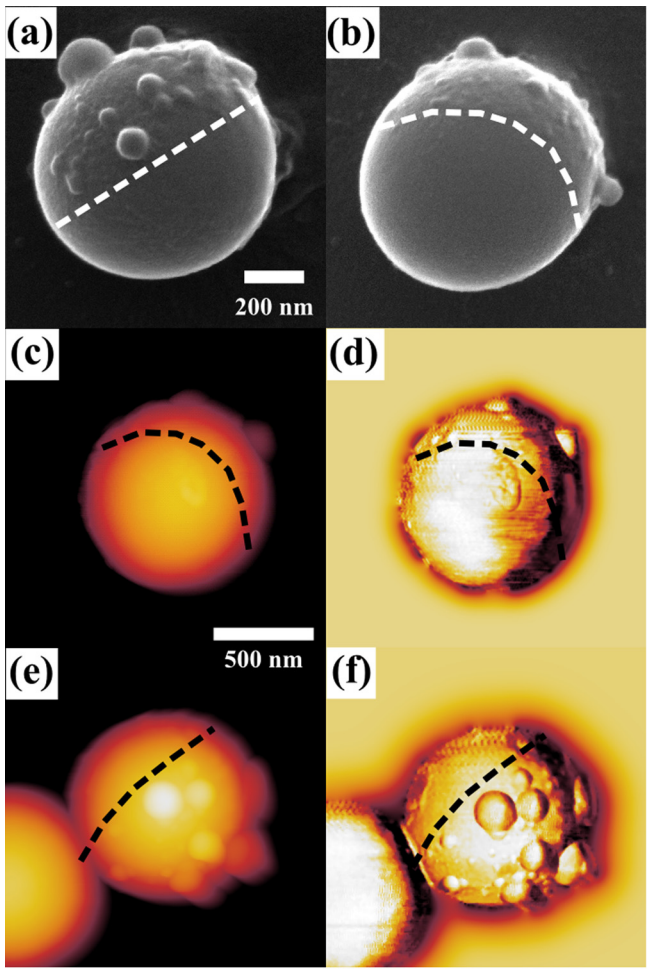

FIG. 5. SEM ((a) and (b)), AFM height ((c) and (e)), and AFM phase ((d) and (f)) images of PMMA/silica Janus particles after removal from substrate via sonication in water. The dotted lines act as guides to the eye, denoting the Janus boundary.

The MAPLE-based Janus particle fabrication scheme presented here has numerous unique advantages. The technique can be used to fabricate patchy Janus particles with innumerable material combinations: a diverse array of inorganic and organic precursor particles can be used as well as a variety of MAPLE-deposited materials. The flexibility of the technique is further augmented by the ability to simply control the Janus anisotropy as well as the surface roughness of the decorating material. We confirmed via AFM and SEM that the particles remain intact with a Janus morphology after sonication into a water suspension. This MAPLE-based Janus particle fabrication technique can enable greater flexibility and control over material properties for applications such as surfactants for emulsion stabilization.

We acknowledge support of the National Science Foundation (NSF) Materials Research Science and Engineering Center program through the Princeton Center for Complex Materials (DMR-0819860) and usage of the PRISM Imaging and Analysis Center at Princeton University. R.D.P. acknowledges partial support from the NSF through a CAREER Award (DMR-1053144) and the AFOSR through a YIP Award (FA9550-12-1-0223). K.B.S. acknowledges support from the Porter Ogden Jacobus fellowship from Princeton University. D.A.C. acknowledges support from the NSF GRFP.

[1]P. G. de Gennes, Science **256**, 495 (1992).
[2]A. Walther and A. H. E. Müller, Chem. Rev. **113**, 5194 (2013).
[3]A. Walther, K. Matussek, and A. H. E. Müller, ACS Nano **2**, 1167 (2008).
[4]N. Glaser, D. J. Adams, A. Böker, and G. Krausch, Langmuir **22**, 5227 (2006).
[5]B. J. Park and D. Lee, ACS Nano **6**, 782 (2012).
[6]A. Walther, M. Hoffmann, and A. H. E. Müller, Angew. Chem. Int. Ed. **47**, 711 (2008).
[7]S. Jiang, Q. Chen, M. Tripathy, E. Luijten, K. S. Schweizer, and S. Granick, Adv. Mater. **22**, 1060 (2010).
[8]J. Yoon, A. Kota, S. Bhaskar, A. Tuteja, and J. Lahann, ACS Appl. Mater. Interfaces **5**, 11281 (2013).
[9]T. Tanaka, M. Okayama, H. Minami, and M. Okubo, Langmuir **26**, 11732 (2010).
[10]J. Choi, Y. Zhao, D. Zhang, S. Chien, and Y.-H. Lo, Nano Lett. **3**, 995 (2003).
[11]R. M. Erb, N. J. Jenness, R. L. Clark, and B. B. Yellen, Adv. Mater. **21**, 4825 (2009).
[12]R. A. Pavlick, S. Sengupta, T. McFadden, H. Zhang, and A. Sen, Angew. Chem. Int. Ed. **50**, 9374 (2011).
[13]M. Yoshida, K.-H. Roh, S. Mandal, S. Bhaskar, D. Lim, H. Nandivada, X. Deng, and J. Lahann, Adv. Mater. **21**, 4920 (2009).
[14]S.-H. Hu and X. Gao, J. Am. Chem. Soc. **132**, 7234 (2010).
[15]A. Alexeev, W. E. Uspal, and A. C. Balazs, ACS Nano **2**, 1117 (2008).
[16]C. Kaewsaneha, P. Tangboriboonrat, D. Polpanich, M. Eissa, and A. Elaissari, ACS Appl. Mater. Interfaces **5**, 1857 (2013).
[17]F. Liang, C. Zhang, and Z. Yang, Adv. Mater. **26**(40), 6944–6949 (2014).
[18]A. B. Pawar and I. Kretzschmar, Langmuir **24**, 355 (2008).
[19]V. N. Paunov and O. J. Cayre, Adv. Mater. **16**, 788 (2004).
[20]X. Y. Ling, I. Y. Phang, C. Acikgoz, M. D. Yilmaz, M. A. Hempenius, G. J. Vancso, and J. Huskens, Angew. Chem. Int. Ed. **48**, 7677 (2009).
[21]R. Sreenivasan and K. K. Gleason, Chem. Vap. Deposition **15**, 77 (2009).
[22]K. B. Shepard and R. D. Priestley, Macromol. Chem. Phys. **214**, 862 (2013).
[23]K. D. Anderson, M. Luo, R. Jakubiak, R. R. Naik, T. J. Bunning, and V. V. Tsukruk, Chem. Mater. **22**, 3259 (2010).
[24]R. T. Chen, B. W. Muir, G. K. Such, A. Postma, K. M. McLean, and F. Caruso, Chem. Commun. **46**, 5121 (2010).
[25]A. H. Gröschel, A. Walther, T. I. Löbling, F. H. Schacher, H. Schmalz, and A. H. E. Müller, Nature **503**, 247 (2013).
[26]B. P. Binks and R. Murakami, Nat. Mater. **5**, 865 (2006).
[27]L. Y. Wu, B. M. Ross, S. Hong, and L. P. Lee, Small **6**, 503 (2010).
[28]A. Piqué, Appl. Phys. A **105**, 517 (2011).
[29]A. Pique, R. A. McGill, D. B. Chrisey, D. Leonhardt, T. E. Mslna, B. J. Spargo, J. H. Callahan, R. W. Vachet, R. Chung, and M. A. Bucaro, Thin Solid Films **355–356**, 536 (1999).
[30]J. Greer, Appl. Phys. A: Mater. Sci. Process. **105**, 661 (2011).
[31]K. B. Shepard, C. B. Arnold, and R. D. Priestley, Appl. Phys. Lett. **103**, 123105 (2013).
[32]B. G. Prevo and O. D. Velev, Langmuir **20**, 2099 (2004).
[33]See supplementary material at http://dx.doi.org/10.1063/1.4913913 for detailed experimental procedures and Janus particle post-annealing data. (n.d.).
[34]K. B. Shepard, C. B. Arnold, and R. D. Priestley, ACS Macro Lett. **3**, 1046 (2014).
[35]H. Rezvantalab and S. Shojaei-Zadeh, Phys. Chem. Chem. Phys. **16**, 8283 (2014).
[36]H. Rezvantalab and S. Shojaei-Zadeh, Langmuir **29**, 14962 (2013).